MOCVD Growth of GaBN on 6H-SiC (0001) Substrates

C.H. WEI,[1] Z.Y. XIE,[1] J.H. EDGAR,[1] K.C. ZENG,[2] J.Y. LIN,[2] H.X. JIANG,[2] J. CHAUDHURI,[3] C. IGNATIEV,[3] and D.N. BRASKI[4]

1.—Kansas State University, Department of Chemical Engineering, Manhattan, KS 66506. 2.—Kansas State University, Department of Physics, Manhattan, KS 66506. 3.—Wichita State University, Department of Mechanical Engineering, Wichita, KS 67260. 4.—Oak Ridge National Laboratory, High Temperature Material Laboratory, Oak Ridge, TN 37831

$B_xGa_{1-x}N$ films were deposited on 6H-SiC (0001) substrates at 1000°C by low pressure MOVPE using diborane, trimethylgallium, and ammonia as precursors. The presence of boron was detected by Auger scanning microprobe, the shift of the (00.2) x-ray diffraction peak, and low-temperature photoluminescence. A single-phase $B_xGa_{1-x}N$ alloy with x = 1.5% was produced at the gas phase B/Ga ratio of 0.005. Phase separation into wurtzite BGaN and the B-rich phase occurred for a B/Ga ratio in the 0.01–0.2 range. Only BN was formed for B/Ga > 0.2. The B-rich phase was identified as h-BN with sp^2 bonding based on the results of Fourier transform infrared spectroscopy. As the diborane flow exceeds the threshold concentration, the growth rate of BGaN decreases sharply, because the growth of GaN is poisoned by the formation of the slow growing BN phase. The bandedge emission of $B_xGa_{1-x}N$ varies from 3.451 eV for x = 0% with FWHM of 39.2 meV to 3.465 eV for x = 1.5% with FWHM of 35.1 meV. The narrower FWHM indicates that the quality of GaN epilayer is improved with a small amount of boron incorporation. The PL linewidths become broader as more boron is introduced into the solid solution.

Key words: GaBN, MOCVD, BN, GaN

INTRODUCTION

GaN has attracted considerable interest for the fabrication of blue/green light emitting diodes (LEDs), blue laser diodes (LDs), and high-power electronic devices. Sapphire is the most commonly employed substrate for GaN growth, but has several shortcomings including a large lattice constant mismatch (~14%),[1] a poor thermal conductivity, and it is electrically insulating. In contrast, 6H-SiC has a smaller lattice mismatch (~3%),[2] a closer thermal expansion coefficient, and a higher thermal conductivity (by a factor of 10) than sapphire. Moreover, SiC is a conductive substrate, which simplifies the fabrication of LEDs or laser structures having a single top and substrate contact.

By adding boron to GaN forming a $B_xGa_{1-x}N$ alloy, it may be possible to reduce or eliminate the lattice constant mismatch between GaN epilayers and 6H-SiC substrates.[3] However, the large disparity of crystal structures between BN and GaN seriously limits the growth of single-phase BGaN alloy. To enhance the boron solubility in GaN, wurtzite BN (w-BN), a metastable structure of BN, is the preferable structure for alloy growth, but hexagonal BN (h-BN) is normally produced by MOCVD or MBE. It is hoped that in alloys with low boron content w-BN can be stabilized by the presence of GaN.

Several groups attempted to grow epitaxial $B_xGa_{1-x}N$ alloys using sapphire as the substrate. A.Y. Polyakov et al. observed that the highest boron solubility in GaN was about 1% at 1000°C by MOVPE.[4] V.K. Gupta et al. reported single crystals $B_xGa_{1-x}N$ with x up to 2% by MBE.[5] In our study, 6H-SiC (0001) was chosen as the substrate, since less boron incorporation ($B_{0.17}Ga_{0.83}N$) would be necessary to eliminate the lattice constant mismatch. In addition, SiC substrates could be more favorable for substitutional incorporation of higher boron in BGaN from elastic energy consideration.[6]
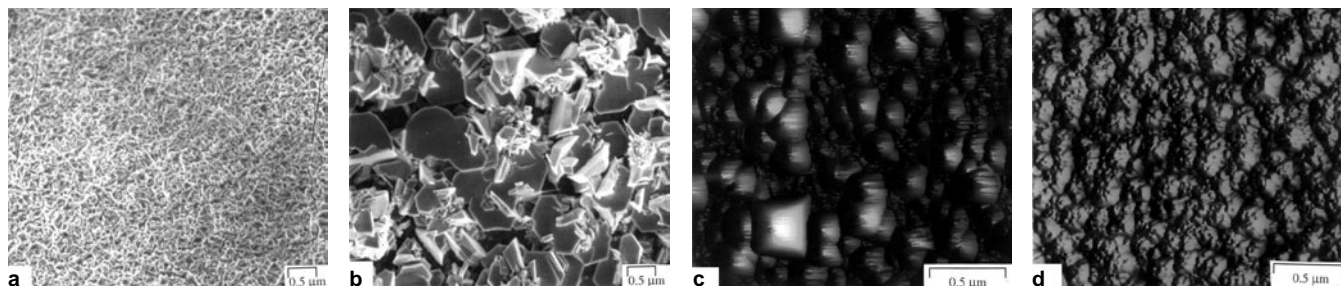
Fig. 1. Surface morphology of BGaN films grown at B/Ga ratio of (a) 0.005; (b) 0.01; (SEM images magnification: 1 kx) (c) 0.05; (d) 0.2 (AFM images).

Another motivation for developing $B_xGa_{1-x}N$ alloys is the possibility of fabricating BGaN-based semiconductor devices. Based on the calculation of Honda et al.,[7] the transparency carrier density of $B_{0.17}Ga_{0.83}N$ is only slightly smaller than that of GaN, which is possibly used in the UV spectral region. Therefore, there is an obvious need to determine how the energy bandgap changes with boron content in BGaN alloys.

In this paper, BGaN films were grown on 6H-SiC by low pressure MOCVD to determine the boron solubility in the single-phase GaN, the ability of reducing the lattice constant mismatch, as well as the effects on the structural and optical properties of GaN. The films were characterized using scanning electron microscopy, atomic force microscopy, scanning Auger microprobe, double-crystal x-ray diffraction, Fourier transform infrared spectroscopy, and photoluminescence.

EXPERIMENTAL PROCEDURE

BGaN films were deposited on the Si face of on-axis 6H-SiC (0001) substrates in a vertical reactor by MOVPE at 76 torr. The 6H-SiC substrates were ultrasonically degreased in sequential baths of trichloroethylene, acetone and methanol, rinsed in deionized water, then dipped into a 10% HF solution to remove the native oxide layer. Prior to growth, the 6H-SiC substrates were annealed in hydrogen at 1100°C for 10 min. Trimethylgallium (TMG) and ammonia (NH_3) were Ga and N source gases with hydrogen as the carrier gas. The boron precursor was 0.01% diborane (B_2H_6) diluted in H_2. A GaN buffer layer with 20–30 nm thickness was first grown at 565°C and ramped to 1000°C in 10 min for crystallization. As the substrate temperature was raised to 1000°C, BGaN films were deposited for 1 h. The low-temperature buffer layer was essential for wetting the 6H-SiC substrates for continuous film growth. The TMG, NH_3, and H_2 were fixed at 18 µmol/min, 1.25, and 1.8 slm, respectively, while the gas phase B/Ga ratio was varied from 0 to 1.

The surface morphology of the samples was examined by scanning electron microscopy (SEM) or atomic force microscopy (AFM). The compositions and phases of films were investigated using a PHI 660 scanning Auger microprobe (SAM) after bombarding the surface with argon ions for several seconds to remove surface contamination. The boron composition x in $B_xGa_{1-x}N$ was calculated by the shift of the GaN (00·2) x-ray diffraction peak applying Vegard's law.[8] Fou-
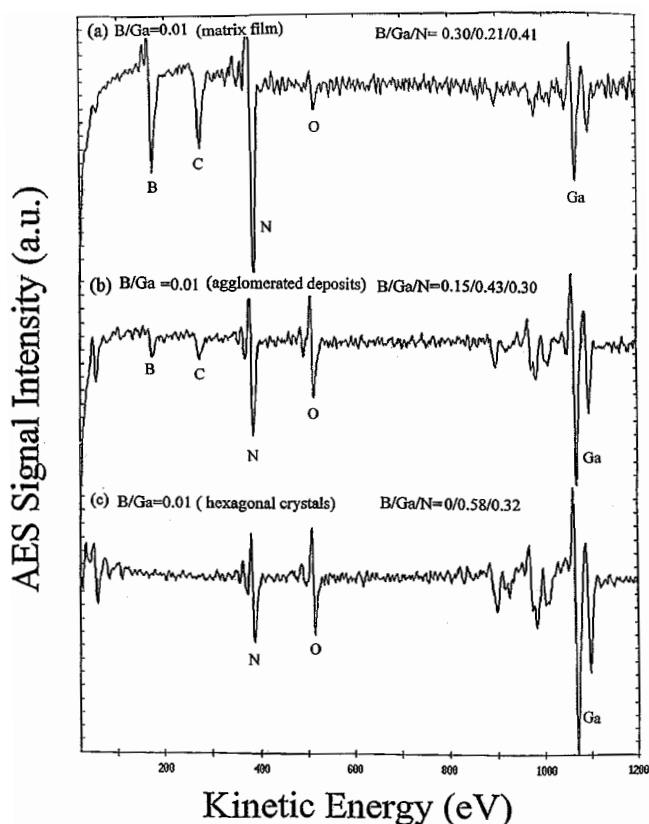

Fig. 2. Auger spectra of BGaN deposited at B/Ga = 0.01.

rier transform infrared (FTIR) spectroscopy was employed to characterize the chemical bonding of B-rich phases. To determine the bandedge emission of the samples, low temperature photoluminescence (PL) spectra were measured by using a picosecond laser spectroscopy system with an average output power of about 20 mW, and a tunable photon energy up to 4.5 eV. Finally, the thickness of the films for the estimation of growth rate was obtained either from cross-sectional SEM for thick films or the argon-ion sputtering rate on thin layers during Auger measurements.

RESULTS AND DISCUSSION

The surface morphology of films grown with gas phase B/Ga ratios of 0.005, 0.01, 0.05, 0.2 at 1000°C are shown in Fig. 1a–d. Apparently, the well-faceted crystals decrease with more boron incorporated into the film. Without adding any boron, the GaN surface
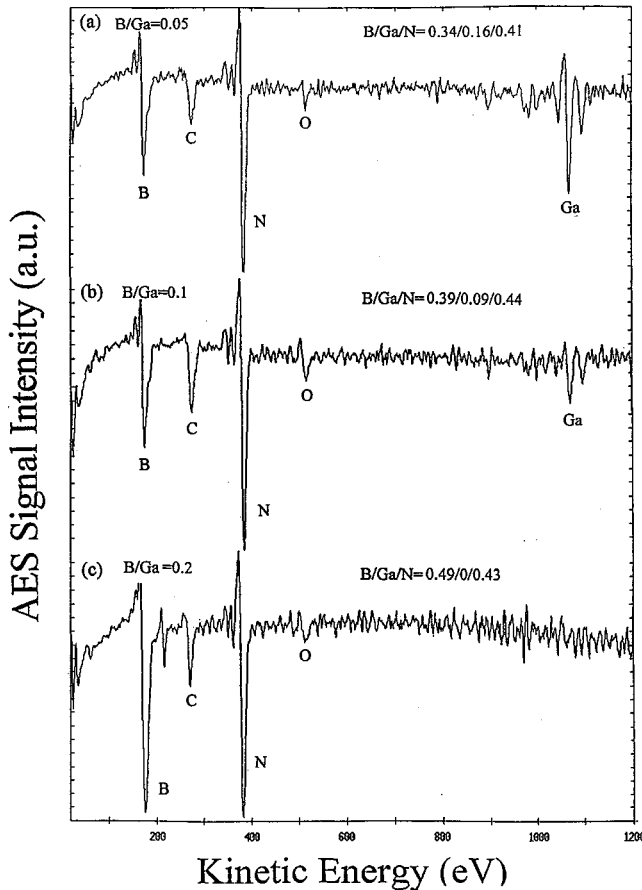
Fig. 3. Auger spectra of samples grown at B/Ga ratio of (a) 0.05; (b) 0.1; (c) 0.2.

Fig. 4. θ-2θ XRD scans of films deposited at different B/Ga ratios. (a) 0.05; (b) 0.01; (c) 0.005.

is specular and mirror-like. However, starting the B/Ga ratio of 0.005 (Fig. 1a), the surface morphology becomes rough and is covered with ridged-like crystals. For further increase in B/Ga ratio to 0.01, the surface displays several distinct features as seen in Fig. 1b: well (00·1) oriented epicrystals with an average size of about 4 μm and smaller agglomerated deposits on top as well as a matrix film around the hexagonal crystals. These suggest that multiple phases with various boron concentrations exist in this sample. As the B/Ga ratio is increased above 0.02, the growth rate drops significantly and the grown layers look shiny, smooth to the eye. AFM images of layers deposited at B/Ga ratio of 0.05 and 0.2 are shown in Fig. 1c and d. The well-faceted crystals disappear and dome-shaped aggregates are observed with an average size of 0.2 μm in Fig. 1c and 0.1 μm in Fig. 1d. The average height of the aggregates in Fig. 1 c is 450 nm and 200 nm in Fig. 1d. These features indicate that the layers are composed of the boron-rich phase, since the dome-shaped growth features are often observed in BN deposition by CVD.[9]

The presence of B in the solid phase was confirmed by Auger measurements. Auger spectra of the films deposited at different B/Ga ratios are presented in Figs. 2 and 3. Only Ga and N peaks were detected for the low B/Ga = 0.005 sample. Since Auger is not sufficiently sensitive to detect the low concentration
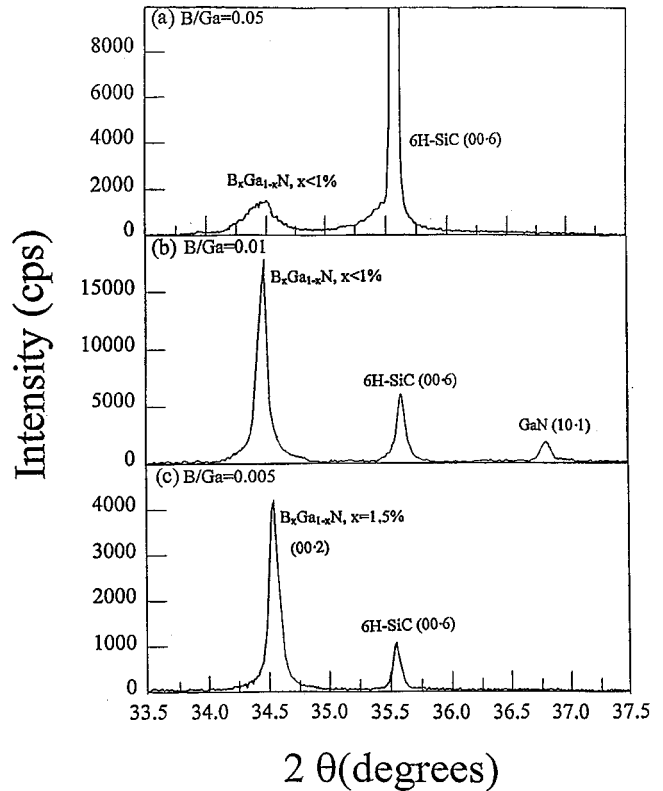
of B (detection limit: 2 atomic %), other measurements such as XRD and PL were used to examine the boron composition in this sample. Next, to verify the existence of multiple phases as seen in Fig. 1b, Auger spectra obtained from three different features are shown in Fig. 2. The matrix film and agglomerated deposits on top reveal formation of the B-rich solid phase, as shown in Fig. 2a and b. However, the well-oriented hexagonal crystals are nearly pure GaN crystals (Fig. 2c). Figure 3 shows Auger spectra of samples grown with higher B/Ga ratios. Clearly, the boron concentration in the solid phase increases with an increase in the diborane flow. Note that as diborane in the gas phase exceeds a certain concentration (B/Ga = 0.2 in Fig. 3c), it completely poisons the growth of GaN and the solid phase contains only BN with no Ga incorporation. Besides the B, Ga, and N main peaks, oxygen and carbon were detected in all samples. We speculate that these impurities originate from the reaction between diborane, ammonia, and methyl groups not from surface contamination, because the amounts of C and O are slightly reduced after Ar ion sputtering.

If all the boron detected by Auger were substitutionally incorporated into GaN, one would expect a significant shift of the GaN (00·2) diffraction peak toward higher 2θ angles. X-ray diffraction pattern for the sample grown with B/Ga = 0.05 is plotted in Fig. 4a. The broad GaN (00·2) peak shows no obvious shift suggesting that the actual composition of $B_xGa_{1-x}N$ corresponds to x less than 1%; the rest of the boron

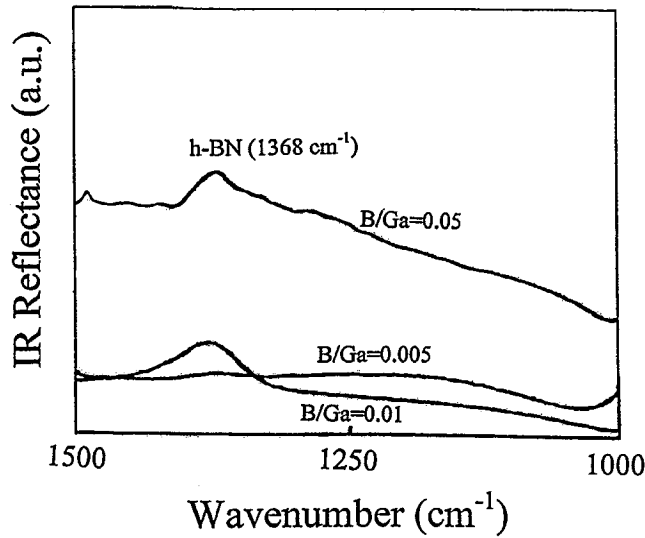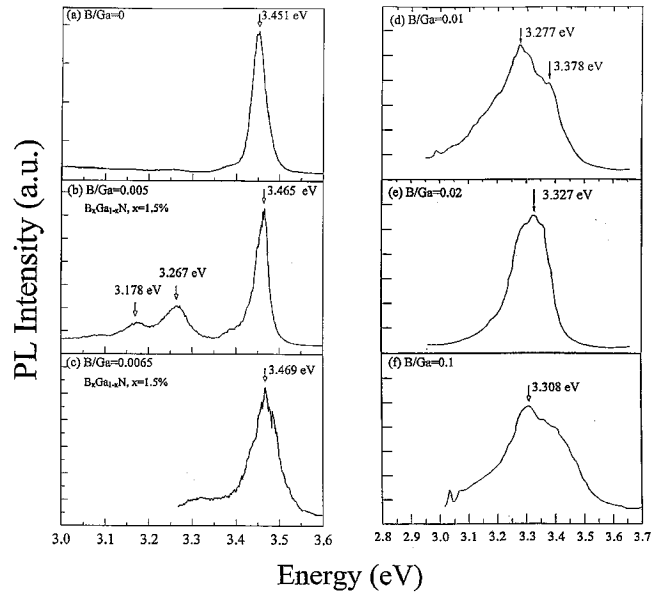Fig. 5. IR reflectance of the films in the 1000–1500 wavenumber (cm⁻¹).

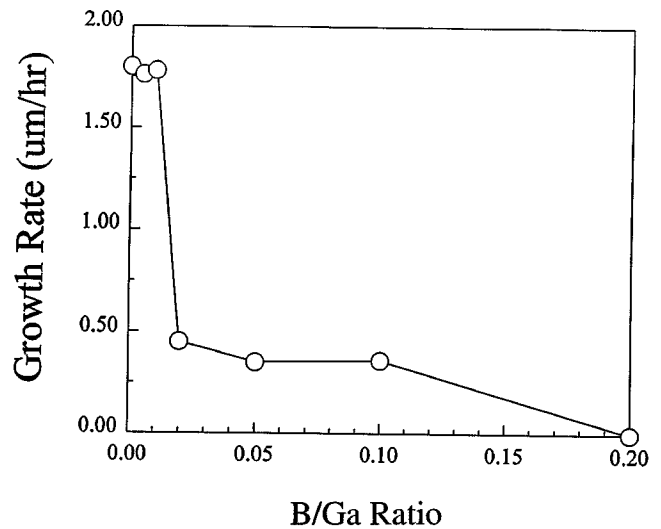Fig. 6. 10 K PL spectra of samples measured at B/Ga ratio (a) 0; (b) 0.005; (c) 0.0065; (d) 0.01; (e) 0.02; (f) 0.1.

Fig. 7. BGaN growth rate as a function of B/Ga ratio.

apparently forming a second boron-rich phase. It is difficult to obtain the x-ray diffraction from the B-rich phase due to the small x-ray cross-section area of boron. However, a very low-intensity, broad hump feature at 25–30° was observed (not shown) and ascribed to the turbostractic BN (t-BN), in which the sp^2 hexagonal rings formed by B and N atoms are irregularly rotated around the c-axis.[10] The XRD pattern of the sample with multiple phases is plotted in Fig. 4b. The high intensity of GaN (00·2) peak arises from the well-oriented hexagonal crystals, while an extra peak centered at 36.84° is from GaN (10·1) reflection, confirming the polycrystalline nature of the film after spinodal decomposition. Eventually, as the B/Ga ratio is lowered to 0.005, the 2θ GaN (00·2) diffraction angle changed from 34.56° to 34.67° indicating the c-lattice constant decreased from 0.5186 nm to 0.5171 nm. This means that the composition of epitaxial B$_x$Ga$_{1-x}$N corresponds to x = 1.5%, and its XRD pattern is shown in Fig. 4c. The large difference in bond lengths between the binary constituents leads to a very low mutual solubility and wide unstable composition region. Therefore the alloy layers are prone to phase separation or spinodal decomposition.[11]

The chemical structure of BN deposits containing sp^2 or sp^3 bonding was studied using FTIR. As seen in Fig. 5, the peak at 1370 cm⁻¹ corresponds to the TO mode of h-BN for films deposited with B/Ga ≥ 0.01.[12] No h-BN sp^2 bonding is observed for the single-phase B$_{0.015}$Ga$_{0.985}$N alloy, most likely because the boron atoms are substitutionally grown into GaN lattice.

Low-temperature (10 K) PL spectra of six samples grown with B/Ga ratio varying from 0 to 0.1 are shown in Figs. 6a–f. The dominant peak in the GaN (x = 0%) PL spectrum centered at 3.451 eV with FWHM of 39.2 meV is attributed to near bandedge emission. The energy of bandedge emission increases from 3.451 eV to 3.465 eV (FWHM = 35.1 meV) with increasing boron composition (x) from 0% to 1.5 % (Fig. 6b). Two emission lines with energy peak positions at 3.267 eV and 3.178 eV are from donor-

acceptor (D-A pair) recombination. The narrower linewidth suggests that the quality of BGaN alloy is improved with a small amount of boron incorporation. From Fig. 6c, although the B/Ga ratio is increased to 0.0065, the boron composition, x, remains unchanged at 1.5% and the bandedge emission occurs at 3.469 eV with broader FWHM compared with Fig. 6b. It appears that the bandedge emission shifts to higher energy with increasing the gas phase diborane concentration. However, as the B/Ga ratio is increased from 0.01 to 0.1, the dominant emission line starts to decline, as seen in Fig. 6d–f. Since these samples are characterized as containing h-BN phase with sp^2 structure, the emission peaks at near 3.3 eV could originate from the bandgap energy of h-BN.[13] Several emission peaks are seen in every PL spectrum due to the compositionally inhomogeneous BGaN layer or from the impurity-related transitions. The broad PL

linewidths indicate poor crystalline quality as more boron is introduced into the solid.

Based on the above, the B/Ga ratio is critical for growing and controlling phases of BGaN. Figure 7 shows the growth rate of BGaN as a function of B/Ga ratio. For a low diborane flow (B/Ga < 0.01), the growth rate is almost unaffected by the presence of boron, and uniform single crystals BGaN alloys can only be produced in this range. When diborane in the gas phase reaches the threshold concentration (B/Ga = 0.02 in this case), the growth of GaN is poisoned by the onset of formation of very slow growing BN phase, causing the growth rate to drop-off. There are regions on the substrate surface not completely covered by BN that can still facilitate the growth of wurtzite GaBN. However, GaN growth on BN surface is hindered by the lacking of active sites protruding from the hexagonal rings of BN, which results in the B-rich phase. This explains the observation of both Ga- and B-rich phases in our sample seen in Fig. 1b. GaN growth is totally poisoned for a high diborane flow (B/Ga > 0.2). Therefore, BGaN growth rate goes down to virtually zero and only BN layer is formed.

CONCLUSIONS

Up to 1.5% B can be substitutionally incorporated into GaN grown on 6H-SiC (0001) substrates at 1000°C by MOCVD. As the diborane flow is increased, the solid solution of BGaN decomposes into wurtzite GaBN and the second B-rich phase. The B-rich phase was characterized as h-BN with sp^2 structure. XRD and PL examinations indicate that higher boron concentration leads to poor crystalline quality and defect formation. However, the film grown with low B/Ga = 0.005 shows higher crystalline quality and narrower PL linewidth compared with the pure GaN sample. PL measurements also display an increase in bandgap energy up to x = 1.5% and then decrease for higher B composition in the films.

REFERENCES

1. I. Akasaki, H. Amano, Y. Koide, K. Hiramatsu, and N. Sawaki, *J. Cryst. Growth* 98, 209 (1989).
2. S. Strite and H. Morkoç, *J. Vac. Sci. Technol. B* 10, 1237 (1992).
3. S. Sakai, Y. Ueta, and Y. Terauchi, *Jpn, J. Appl. Phys.* 32, 4413 (1993).
4. A.Y. Polyakov, M. Shin, M. Skowronski, D.W. Greve, R.G. Wilson, A.V. Govorkov, and R.M. Desrosiers, *J. Electron. Mater.* 26, 237 (1997).
5. V.K. Gupta, C.C. Wamsley, M.W. Koch, and G.W. Wicks *J. Vac. Sci. & Technol. B* 17, 1246 (1999).
6. Alex Zunger, *Handbook of Crystal Growth*, ed. D.T.J. Hurle, Vol. 3. (Amsterdam, the Netherlands: Elsevier, 1994), p. 999.
7. T. Honda, M. Tsubamoto, Y. Kuga, and H. Kawanishi, *Mater. Res. Soc. Symp. Proc.* 482, 1125 (1998).
8. L. Vegard, *Z. Phys.* 5, 17 (1921).
9. W.Y. Lee, W.J. Lackey, P.K. Agrawal, and G.B. Freeman, *J. Amer. Ceram. Soc.* 74, 2649 (1992).
10. J. Thomas, Jr., N.E. Weston, and T.E. O'Connor, *J. Amer. Chem. Soc.* 84, 4619 (1963).
11. C.H. Wei and J.H. Edgar, *J. Cryst. Growth* 208, 179 (1999).
12. S. Hirano, T. Yogo, S. Asada, and S. Naka, *J. Amer. Ceram. Soc.* 72, 66 (1989).
13. G.L. Doll, *Properties of Group III Nitrides*, ed. J.H. Edgar, (London: INSPEC, 1994), p. 169.